

## Evidence for muon neutrino oscillation in an accelerator-based experiment

E. Aliu,<sup>1</sup> S. Andringa,<sup>1</sup> S. Aoki,<sup>10</sup> J. Argyriades,<sup>3</sup> K. Asakura,<sup>10</sup> R. Ashie,<sup>30</sup> H. Berns,<sup>33</sup> H. Bhang,<sup>20</sup> A. Blondel,<sup>26</sup> S. Borghi,<sup>26</sup> J. Bouchez,<sup>3</sup> J. Burguet-Castell,<sup>32</sup> D. Casper,<sup>28</sup> C. Cavata,<sup>3</sup> A. Cervera,<sup>26</sup> K. O. Cho,<sup>4</sup> J. H. Choi,<sup>4</sup> U. Dore,<sup>19</sup> X. Espinal,<sup>1</sup> M. Fechner,<sup>3</sup> E. Fernandez,<sup>1</sup> Y. Fukuda,<sup>15</sup> J. Gomez-Cadenas,<sup>32</sup> R. Gran,<sup>33</sup> T. Hara,<sup>10</sup> M. Hasegawa,<sup>12</sup> T. Hasegawa,<sup>22</sup> K. Hayashi,<sup>12</sup> Y. Hayato,<sup>7</sup> R. L. Helmer,<sup>25</sup> J. Hill,<sup>23</sup> K. Hiraide,<sup>12</sup> J. Hosaka,<sup>30</sup> A. K. Ichikawa,<sup>7</sup> M. Inuma,<sup>8</sup> A. Ikeda,<sup>17</sup> T. Inagaki,<sup>12</sup> T. Ishida,<sup>7</sup> K. Ishihara,<sup>30</sup> T. Ishii,<sup>7</sup> M. Ishitsuka,<sup>31</sup> Y. Itow,<sup>30</sup> T. Iwashita,<sup>7</sup> H. I. Jang,<sup>4</sup> E. J. Jeon,<sup>20</sup> I. S. Jeong,<sup>4</sup> K. Joo,<sup>20</sup> G. Jover,<sup>1</sup> C. K. Jung,<sup>23</sup> T. Kajita,<sup>31</sup> J. Kameda,<sup>30</sup> K. Kaneyuki,<sup>31</sup> I. Kato,<sup>12</sup> E. Kearns,<sup>2</sup> D. Kerr,<sup>23</sup> C. O. Kim,<sup>11</sup> M. Khabibullin,<sup>9</sup> A. Khotjantsev,<sup>9</sup> D. Kielczewska,<sup>34,21</sup> J. Y. Kim,<sup>4</sup> S. Kim,<sup>20</sup> P. Kitching,<sup>25</sup> K. Kobayashi,<sup>23</sup> T. Kobayashi,<sup>7</sup> A. Konaka,<sup>25</sup> Y. Koshio,<sup>30</sup> W. Kropp,<sup>28</sup> J. Kubota,<sup>12</sup> Yu. Kudenko,<sup>9</sup> Y. Kuno,<sup>18</sup> T. Kutter,<sup>27,13</sup> J. Learned,<sup>29</sup> S. Likhoded,<sup>2</sup> I. T. Lim,<sup>4</sup> P. F. Loverre,<sup>19</sup> L. Ludovici,<sup>19</sup> H. Maesaka,<sup>12</sup> J. Mallet,<sup>3</sup> C. Mariani,<sup>19</sup> T. Maruyama,<sup>7</sup> S. Matsuno,<sup>29</sup> V. Matveev,<sup>9</sup> C. Mauger,<sup>21</sup> K. McConnel,<sup>14</sup> C. McGrew,<sup>23</sup> S. Mikheyev,<sup>9</sup> A. Minamino,<sup>30</sup> S. Mine,<sup>28</sup> O. Mineev,<sup>9</sup> C. Mitsuda,<sup>30</sup> M. Miura,<sup>30</sup> Y. Moriguchi,<sup>10</sup> T. Morita,<sup>12</sup> S. Moriyama,<sup>30</sup> T. Nakadaira,<sup>12</sup> M. Nakahata,<sup>30</sup> K. Nakamura,<sup>7</sup> I. Nakano,<sup>17</sup> T. Nakaya,<sup>12</sup> S. Nakayama,<sup>31</sup> T. Namba,<sup>30</sup> R. Nambu,<sup>30</sup> S. Nawang,<sup>8</sup> K. Nishikawa,<sup>12</sup> K. Nitta,<sup>7</sup> F. Nova,<sup>1</sup> P. Novella,<sup>32</sup> Y. Obayashi,<sup>30</sup> A. Okada,<sup>31</sup> K. Okumura,<sup>31</sup> S. M. Oser,<sup>27</sup> Y. Oyama,<sup>7</sup> M. Y. Pac,<sup>5</sup> F. Pierre,<sup>3</sup> A. Rodriguez,<sup>1</sup> C. Saji,<sup>31</sup> M. Sakuda,<sup>7,17</sup> F. Sanchez,<sup>1</sup> A. Sarrat,<sup>23</sup> T. Sasaki,<sup>12</sup> K. Scholberg,<sup>6,14</sup> R. Schroeter,<sup>26</sup> M. Sekiguchi,<sup>10</sup> E. Sharkey,<sup>23</sup> M. Shiozawa,<sup>30</sup> K. Shiraiishi,<sup>33</sup> G. Sitjes,<sup>32</sup> M. Smy,<sup>28</sup> H. Sobel,<sup>28</sup> J. Stone,<sup>2</sup> L. Sulak,<sup>2</sup> A. Suzuki,<sup>10</sup> Y. Suzuki,<sup>30</sup> T. Takahashi,<sup>8</sup> Y. Takenaga,<sup>31</sup> Y. Takeuchi,<sup>30</sup> K. Taki,<sup>30</sup> Y. Takubo,<sup>18</sup> N. Tamura,<sup>16</sup> M. Tanaka,<sup>7</sup> R. Terri,<sup>23</sup> S. T'Jampens,<sup>3</sup> A. Tornero-Lopez,<sup>32</sup> Y. Totsuka,<sup>7</sup> S. Ueda,<sup>12</sup> M. Vagins,<sup>28</sup> C.W. Walter,<sup>6</sup> W. Wang,<sup>2</sup> R.J. Wilkes,<sup>33</sup> S. Yamada,<sup>9</sup> S. Yamamoto,<sup>12</sup> C. Yanagisawa,<sup>23</sup> N. Yershov,<sup>9</sup> H. Yokoyama,<sup>24</sup> M. Yokoyama,<sup>12</sup> J. Yoo,<sup>20</sup> M. Yoshida,<sup>18</sup> and J. Zalipska<sup>21</sup>

(The K2K Collaboration)

<sup>1</sup>*Institut de Fisica d'Altes Energies, Universitat Autònoma de Barcelona, E-08193 Bellaterra (Barcelona), Spain*

<sup>2</sup>*Department of Physics, Boston University, Boston, Massachusetts 02215, USA*

<sup>3</sup>*DAPNIA, CEA Saclay, 91191 Gif-sur-Yvette Cedex, France*

<sup>4</sup>*Department of Physics, Chonnam National University, Kwangju 500-757, Korea*

<sup>5</sup>*Department of Physics, Dongshin University, Naju 520-714, Korea*

<sup>6</sup>*Department of Physics, Duke University, Durham, North Carolina 27708, USA*

<sup>7</sup>*High Energy Accelerator Research Organization(KEK), Tsukuba, Ibaraki 305-0801, Japan*

<sup>8</sup>*Graduate School of Advanced Sciences of Matter, Hiroshima University, Higashi-Hiroshima, Hiroshima 739-8530, Japan*

<sup>9</sup>*Institute for Nuclear Research, Moscow 117312, Russia*

<sup>10</sup>*Kobe University, Kobe, Hyogo 657-8501, Japan*

<sup>11</sup>*Department of Physics, Korea University, Seoul 136-701, Korea*

<sup>12</sup>*Department of Physics, Kyoto University, Kyoto 606-8502, Japan*

<sup>13</sup>*Department of Physics and Astronomy, Louisiana State University, Baton Rouge, Louisiana 70803-4001, USA*

<sup>14</sup>*Department of Physics, Massachusetts Institute of Technology, Cambridge, Massachusetts 02139, USA*

<sup>15</sup>*Department of Physics, Miyagi University of Education, Sendai 980-0845, Japan*

<sup>16</sup>*Department of Physics, Niigata University, Niigata, Niigata 950-2181, Japan*

<sup>17</sup>*Department of Physics, Okayama University, Okayama, Okayama 700-8530, Japan*

<sup>18</sup>*Department of Physics, Osaka University, Toyonaka, Osaka 560-0043, Japan*

<sup>19</sup>*University of Rome La Sapienza and INFN, I-000185 Rome, Italy*

<sup>20</sup>*Department of Physics, Seoul National University, Seoul 151-747, Korea*

<sup>21</sup>*A. Soltan Institute for Nuclear Studies, 00-681 Warsaw, Poland*

<sup>22</sup>*Research Center for Neutrino Science, Tohoku University, Sendai, Miyagi 980-8578, Japan*

<sup>23</sup>*Department of Physics and Astronomy, State University of New York, Stony Brook, New York 11794-3800, USA*

<sup>24</sup>*Department of Physics, Tokyo University of Science, Noda, Chiba 278-0022, Japan*

<sup>25</sup>*TRIUMF, Vancouver, British Columbia V6T 2A3, Canada*

<sup>26</sup>*DPNC, Section de Physique, University of Geneva, CH1211, Geneva 4, Switzerland*

<sup>27</sup>*Department of Physics & Astronomy, University of British Columbia, Vancouver, British Columbia V6T 1Z1, Canada*

<sup>28</sup>*Department of Physics and Astronomy, University of California, Irvine, Irvine, California 92697-4575, USA*

<sup>29</sup>*Department of Physics and Astronomy, University of Hawaii, Honolulu, Hawaii 96822, USA*

<sup>30</sup>*Kamioka Observatory, Institute for Cosmic Ray Research, University of Tokyo, Kamioka, Gifu 506-1205, Japan*

<sup>31</sup>*Research Center for Cosmic Neutrinos, Institute for Cosmic Ray Research, University of Tokyo, Kashiwa, Chiba 277-8582, Japan*

<sup>32</sup>*Instituto de Física Corpuscular, E-46071 Valencia, Spain*

<sup>33</sup>*Department of Physics, University of Washington, Seattle, Washington 98195-1560, USA*

<sup>34</sup>*Institute of Experimental Physics, Warsaw University, 00-681 Warsaw, Poland*

(Dated: November 10, 2004)

We present results for  $\nu_\mu$  oscillation in the KEK to Kamioka (K2K) long-baseline neutrino oscillation experiment. K2K uses an accelerator-produced  $\nu_\mu$  beam with a mean energy of 1.3 GeV directed at the Super-Kamiokande detector 250 km away. The data sample is  $8.9 \times 10^{19}$  protons on target. In total, 107 events are observed in Super-Kamiokande; we expect  $151_{-10}^{+12}$  if  $\nu_\mu$  does not oscillate. The neutrino energy spectrum distortion caused by  $\nu_\mu$  oscillation is also seen. The probability that we would observe these results if there is no neutrino oscillation is 0.0050% ( $4.0\sigma$ ).

PACS numbers: 14.60.Pq,13.15.+g,25.30.Pt,95.55.Vj

Recent atmospheric [1, 2, 3], reactor [4], and solar neutrino [5, 6] experiments show that the existence of neutrino oscillation and non-zero neutrino mass are very likely. An up/down asymmetry in the zenith angle distribution and a dip in the L/E distribution for atmospheric neutrinos observed in Super-Kamiokande suggest  $\nu_\mu$  to  $\nu_\tau$  oscillation with a mass squared difference ( $\Delta m^2$ ) around  $2.5 \times 10^{-3} \text{eV}^2$  and a mixing angle parameter ( $\sin^2 2\theta$ ) that is almost unity [1, 7].

The KEK to Kamioka long-baseline neutrino oscillation experiment (K2K) [8, 9] is the first accelerator based project to explore neutrino oscillation in the same  $\Delta m^2$  region as atmospheric neutrinos. The neutrino beam is 98%  $\nu_\mu$ , whose direction is monitored every beam spill by measuring the profile of muons from the pion decays. The neutrino beam energy spectrum and profile are measured by the near neutrino detectors (ND) located 300 m from the production target. The ND consists of two detector sets: a 1 kiloton water Cherenkov detector (1KT) and a fine grained detector (FGD) system. The far detector is Super-Kamiokande (SK), a 50 kiloton water Cherenkov detector, located 250 km from KEK.

In this letter, we present evidence for the energy-dependent disappearance of  $\nu_\mu$ , which are presumed to have oscillated to  $\nu_\tau$ . We observe a distortion of the neutrino energy ( $E_\nu$ ) spectrum and a deficit in the total number of events. The expectation for these are derived from measurements at the ND and transformed using the energy-dependent ratio of the  $\nu_\mu$  flux at the far and near detectors (F/N ratio). The F/N ratio accounts for the difference between the small portion of the beam near the center seen by SK and the large section of the beam seen by the ND. This is calculated using the neutrino beam Monte Carlo (MC) simulation and confirmed by measurements of pions from the production target [8, 9].

We have analyzed data taken from June 1999 to February 2004, which corresponds to  $8.9 \times 10^{19}$  protons on target (POT). From 1999 to 2001 (called K2K-I and SK-I), the inner detector surface of SK had 11,146 20-inch photo-multiplier tubes (PMTs) covering 40% of the total area [10]. The FGD was comprised of a scintillating fiber and water detector (SciFi) [11, 12], a lead glass calorimeter (LG), and a muon range detector (MRD) [13].

Starting from January 2003 (K2K-II and SK-II), 19% of the SK inner detector is covered using 5182 PMTs, each enclosed in a fiber reinforced plastic shell with an

acrylic cover. The transparency and reflection of these covers in water are 97% and 1% respectively. The FGD data from this period include  $2.3 \times 10^{19}$  POT without the LG (K2K-IIa), and then  $1.9 \times 10^{19}$  POT (K2K-IIb) with a fully-active scintillator detector (SciBar) [14] in place of the LG. Adding this K2K-II data almost doubles the statistics compared to the previous analysis [9]. The neutrino beam direction is monitored using neutrino events in the MRD. It is stable, within 1 mrad throughout the entire experimental period. Also, these events confirm that the energy spectrum is stable.

The 1KT data alone is used to estimate the expected total number of events at SK because the 1KT uses the same water target and the uncertainties in the neutrino cross section cancel. The event selection and the 25 ton fiducial volume are the same as in [9]. In order to estimate the  $E_\nu$  spectrum along with the other near detectors, we select the subset of events in which all the energy is deposited in the inner detector (fully contained, FC) and only one, muon-like Cherenkov ring is reconstructed (1-ring  $\mu$ -like events). For these events we measure both the muon momentum ( $p_\mu$ ) and angle ( $\theta_\mu$ ), from which we estimate the neutrino energy. For the energy spectrum measurement, the largest contribution to the systematic uncertainty is +2/-3% in the overall energy scale.

The SciFi detector is made of layers of scintillating fibers between tanks of aluminum filled with water. The fiducial volume is 5.6 tons. The K2K-I analysis includes events which reach the MRD and also events in which the muon track stops in the lead glass, with momentum as low as 400 MeV/c, significantly lowering the energy threshold compared to [9]. The muon momentum threshold for K2K-IIa is 550 MeV/c because in this case we restrict our analysis to events which have hit at least two layers in the MRD to improve the purity of muons.

The SciBar detector consists of 14,848 extruded scintillator strips read out by wavelength shifting fibers and multi-anode PMTs. Strips with dimensions of  $1.3 \times 2.5 \times 300 \text{ cm}^3$  are arranged in 64 layers. Each layer consists of two planes to measure horizontal and vertical position. The scintillator also acts as the neutrino interaction target; it is a fully active detector and has high efficiency for low momentum particles. The size of the detector is  $3 \times 3 \times 1.7 \text{ m}^3$  and the total weight is 15 tons. Although the target is not water, possible differences due to nuclear effects are included in the systematic uncertainty.

TABLE I: The quasi-elastic (QE) efficiency and purity for each sub-sample used in the spectrum analysis. Values without parentheses represent QE reconstruction efficiency [%] out of all QE events in the fiducial volume, and values within parentheses represent QE purity [%] for each sub-sample.

	1-track or	2-track		Total
	1-ring $\mu$ like	QE	non-QE	
1KT	53 (59)	—	—	53
SciFi I	39 (50)	5 (53)	2 (11)	46
SciFi IIa	36 (57)	5 (58)	2 (12)	42
SciBar	51 (57)	15 (72)	4 (17)	70
SK	86 (58)	—	—	86

In SciBar, tracks which traverse at least three layers ( $\sim 8$  cm) are reconstructed. The reconstruction efficiency for an isolated track longer than 10 cm is 99%. In the present analysis, we select charged current (CC) events by requiring at least one of the tracks start from the 9.38 ton fiducial volume and extend to the MRD. With this requirement, the  $p_\mu$  threshold is 450 MeV/c. The  $p_\mu$  scale uncertainty,  $p_\mu$  resolution, and  $\theta_\mu$  resolution are 2.7%, 80 MeV/c, and  $1.6^\circ$ , respectively. The efficiency for a second, short track is lower than that for a muon track mainly due to the overlap with the primary track. This efficiency smoothly increases from the threshold (8 cm, corresponding to 450 MeV/c proton) and reaches 90% at 30 cm (670 MeV/c for proton).

For SciFi and SciBar, we select events in which one or two tracks are reconstructed. For two-track events, we use kinematic information to discriminate between quasi-elastic (QE) and non-QE interactions. The direction of the recoil proton can be predicted from  $p_\mu$  and  $\theta_\mu$  assuming a QE interaction. If the difference between the observed and the predicted direction of the second track is within  $25^\circ$ , the event is in the QE enriched sample. Events for which this difference is more than  $30^\circ$  ( $25^\circ$ ) for SciFi (SciBar) are put into the non-QE sample. The QE efficiency and purity of the samples are estimated from the MC simulation and are summarized in Tab. I.

We measure the  $E_\nu$  spectrum at the ND by fitting the two-dimensional distributions of  $p_\mu$  versus  $\theta_\mu$  with a baseline MC expectation [9]. We simultaneously obtain the cross section ratio of non-QE to QE interactions ( $R_{\text{nqe}}$ ) relative to our MC simulation. However, we observe a significant deficit of forward going muons in all ND data compared to the MC. To avoid a bias due to this, we perform the  $E_\nu$  fit using only data with  $\theta_\mu > 20(10)$  degrees for 1KT (SciFi and SciBar). The  $\chi^2$  value at the best fit is 538.5 for 479 degrees of freedom (DOF). The resulting  $E_\nu$  spectrum and its error are summarized in Tab. II, while the best fit value of  $R_{\text{nqe}}$  is 0.95.

Muons in the forward direction also correspond to events with a low value for the square of the momentum transfer ( $q^2$ ), the relevant parameter in the neutrino in-

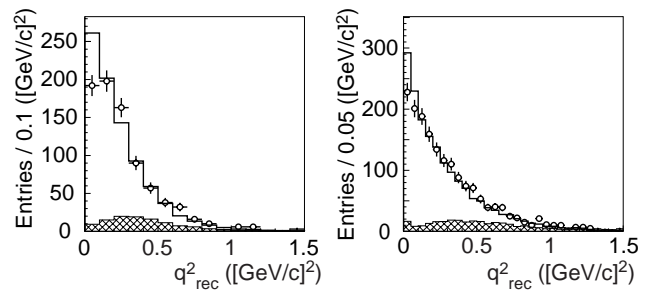


FIG. 1: Reconstructed  $q^2$  distributions for 2-track nonQE-enhanced samples of SciFi (left) and SciBar (right). Open circles with error bars are data, solid lines are MC predictions, and hatched areas show CC-QE component estimated from MC simulation. A clear deficit is observed in the low  $q^2$  region.

teraction models. From inspection of all subsamples, the amount of resonant pion production and coherent pion production at low  $q^2$  in the MC simulation are possible sources of the forward muon deficit. In our MC, we use the model for resonant pion by Rein and Sehgal [15] with axial vector mass of 1.1 GeV/c<sup>2</sup>. For coherent pion, we use the model by Rein and Sehgal [16] with the cross section calculated by Marteau et al. [17]. Figure 1 shows the  $q^2$  distributions calculated from  $p_\mu$  and  $\theta_\mu$  assuming CC-QE kinematics ( $q_{\text{rec}}^2$ ). We modify the MC simulation used in the near and the far detector analysis to account for the effect of the observed deficit. For resonant pions, we suppress the cross section by  $q^2/A$  for  $q^2 < A$  and leave it unchanged for  $q^2 > A$ . From a fit to the SciBar 2-track non-QE sample,  $A$  is  $0.10 \pm 0.03$  (GeV/c)<sup>2</sup>. Alternatively, if we assume that the source of the low  $q^2$  deficit is coherent pion production, we find the observed distribution is reproduced best with zero coherent pion.

Considering both possibilities mentioned above, we fit the parameter  $R_{\text{nqe}}$  again and check the agreement with the data. The  $E_\nu$  spectrum is kept fixed at the values already obtained in the first step, but now we use data at all angles. The best fit value for  $R_{\text{nqe}}$  is 1.02 (1.06) with  $\chi^2/\text{DOF}$  of 638.1/609 (667.1/606) when we suppress resonant pion (eliminate the coherent pion). The  $p_\mu$  and  $\theta_\mu$  distributions from all detectors are well reproduced for both cases with reasonable  $\chi^2$ , as shown in Fig. 2. If we repeat the fit with the  $E_\nu$  spectrum free, the results are still consistent with the first step. Examining these results carefully, we conclude that we cannot identify which is the source of the observed deficit in the low  $q^2$  region. Because the value of  $R_{\text{nqe}}$  changes depending on the choice of model, an additional systematic error of 0.1 is assigned to  $R_{\text{nqe}}$ . For the oscillation analysis presented in this letter, we choose to suppress the resonance production mode in the MC simulation and when we determine the central value of  $R_{\text{nqe}}$ . However, we find that the final oscillation results do not change if we instead choose to eliminate coherent pion.

TABLE II: The  $E_\nu$  spectrum fit results.  $\Phi_{\text{ND}}$  is the best fit value of flux for each  $E_\nu$  bin. It is given relative to the 1.0–1.5 GeV bin. The percentages of uncertainties in  $\Phi_{\text{ND}}$ , F/N ratio, and reconstruction efficiencies of SK-I and SK-II are also shown.

$E_\nu$ (GeV)	$\Phi_{\text{ND}}$	$\Delta(\Phi_{\text{ND}})$	$\Delta(\text{F/N})$	$\Delta(\epsilon_{\text{SK-I}})$	$\Delta(\epsilon_{\text{SK-II}})$
0.0 – 0.5	0.032	46	2.6	3.7	4.5
0.5 – 0.75	0.32	8.5	4.3	3.0	3.2
0.75 – 1.0	0.73	5.8	4.3	3.0	3.2
1.0 – 1.5	$\equiv 1$	—	4.9	3.3	8.2
1.5 – 2.0	0.69	4.9	10	4.9	7.8
2.0 – 2.5	0.34	6.0	11	4.9	7.4
2.5 – 3.0	0.12	13	12	4.9	7.4
3.0 –	0.049	17	12	4.9	7.4

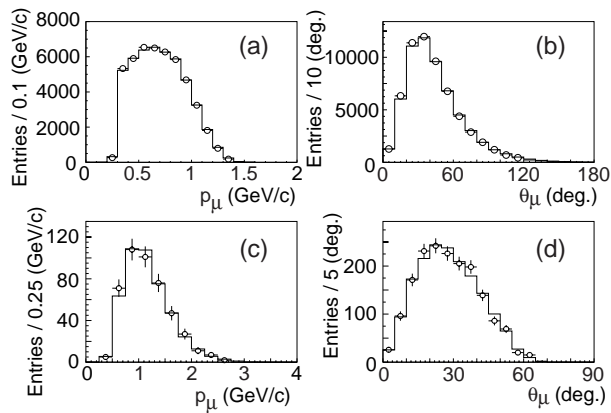


FIG. 2: A selection of muon momentum ( $p_\mu$ ) and direction ( $\theta_\mu$ ) distributions: (a) the  $p_\mu$  distribution of 1KT FC 1-ring  $\mu$ -like sample, (b) 1KT  $\theta_\mu$  for the same sample, (c) SciFi  $p_\mu$  for 2-track QE sample, and (d) SciBar  $\theta_\mu$  for 2-track nonQE sample. Open circles represent data, while histograms are MC predictions using the best fit  $E_\nu$  spectrum and suppression of the resonant pion production.

Events in SK from the accelerator are selected based on timing information from the global positioning system. The background coming from atmospheric neutrinos is estimated to be  $2 \times 10^{-3}$  events. For K2K-I+II there are 107 events in the 22.5 kiloton fiducial volume that are fully contained, have no energy seen in the outer detector, and have at least 30 MeV deposited in the inner detector. The expected number of FC events at SK without oscillation is  $151^{+12}_{-10}(\text{syst})$ . The major contributions to the errors come from the uncertainties in the F/N ratio (5.1%) and the normalization (5.1%); the latter is dominated by the uncertainty in the fiducial volumes due to the vertex reconstruction at both 1KT and SK.

We reconstruct the neutrino energy ( $E_\nu^{\text{rec}}$ ), assuming CC-QE kinematics, from  $p_\mu$  and  $\theta_\mu$  for the 57 events in the 1-ring  $\mu$ -like subset of the SK data. With these we measure the energy spectrum distortion caused by neutrino oscillation. The detector systematics of SK-I and

SK-II are slightly different because of the change in the number of inner detector PMTs. The main contribution to the systematic error of the oscillation analysis based on the energy spectrum is the energy scale uncertainty: 2.0% for SK-I and 2.1% for SK-II. Uncertainties for the ring counting and particle identification are estimated using the atmospheric neutrino data sample and MC simulation. The differences between the K2K and atmospheric neutrino fluxes are also taken into account.

A two-flavor neutrino oscillation analysis, with  $\nu_\mu$  disappearance, is performed using a maximum-likelihood method. The oscillation parameters,  $(\sin^2 2\theta, \Delta m^2)$ , are estimated by maximizing the product of the likelihood for the observed number of FC events ( $\mathcal{L}_{\text{num}}$ ) and that for the shape of the  $E_\nu^{\text{rec}}$  spectrum ( $\mathcal{L}_{\text{shape}}$ ). The probability density function (PDF) for  $\mathcal{L}_{\text{num}}$  is the Poisson probability for the expected number of events. The PDF for  $\mathcal{L}_{\text{shape}}$  is the expected  $E_\nu^{\text{rec}}$  distribution at SK, which is estimated from the MC simulation. The PDFs are defined for K2K-I and K2K-II separately. The systematic uncertainties due to the following sources are taken into account in the PDFs: the  $E_\nu$  spectrum measured by the ND, the F/N ratio, the reconstruction efficiency and absolute energy scale of SK, the ratio of neutral current to CC-QE cross section, the ratio of CC non-QE to CC-QE cross section and the overall normalization. The systematic uncertainties modify the expected distributions, and each is assumed to follow a Gaussian distribution [7]. A constraint term ( $\mathcal{L}_{\text{syst}}$ ) is multiplied with the likelihood for each of these systematics, and  $\mathcal{L}_{\text{num}} \times \mathcal{L}_{\text{shape}} \times \mathcal{L}_{\text{syst}}$  is maximized during the fit. The total number of parameters varied in the fit is thirty-four.

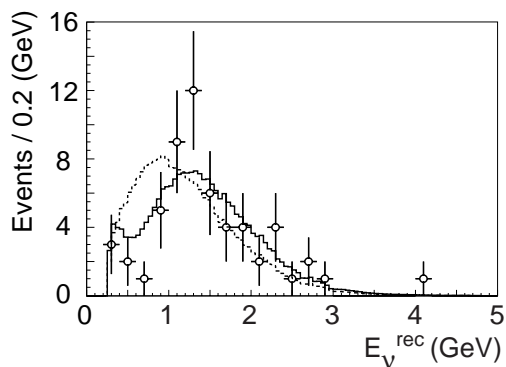


FIG. 3: The reconstructed  $E_\nu$  distribution for the SK 1-ring  $\mu$ -like sample. Points with error bars are data. The solid line is the best fit spectrum. The dashed line is the expected spectrum without oscillation. These histograms are normalized by the number of events observed (57).

The best fit point within the physical region is  $(\sin^2 2\theta, \Delta m^2) = (1.0, 2.8 \times 10^{-3} \text{ eV}^2)$ . The expected number of events at this point is 103.8, which agrees well with the 107 observed. The best fit  $E_\nu$  distribution is shown with the data in Fig. 3. The consistency between the observed

and fit  $E_\nu$  distributions is checked using a Kolmogorov-Smirnov (KS) test. For the best fit parameters, the KS probability is 36%, while that for the no-oscillation hypothesis is 0.08%. The highest likelihood is at a point  $(1.5, 2.2 \times 10^{-3} \text{ eV}^2)$  which is outside of the physical region. The probability that we would get  $\sin^2 2\theta \geq 1.5$  if the true parameters are our best fit physical parameters is 13%, based on MC virtual experiments. For the rest of this letter we refer only to the physical region best fit. The fit results for all the systematic parameters are reasonable. The fits for the K2K-I and K2K-II sub-samples are consistent with the result for the whole sample.

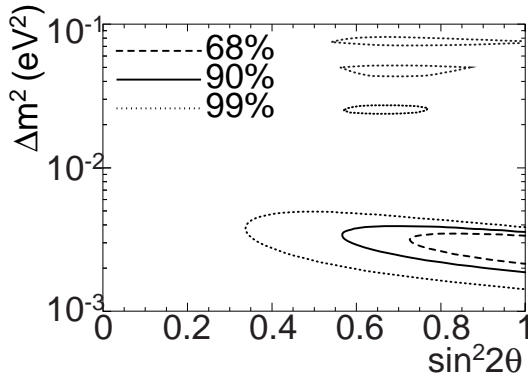


FIG. 4: Allowed regions of oscillation parameters. Dashed, solid and dot-dashed lines are 68.4%, 90% and 99% C.L. contours, respectively.

The possibility that the observations are due to a statistical fluctuation instead of neutrino oscillation is estimated by computing the likelihood ratio of the no-oscillation case to the best fit point. If there is no oscillation, the probability of this result is 0.0050% ( $4.0\sigma$ ). When only normalization (shape) information is used, the probability is 0.26% (0.74%).

Allowed regions for the oscillation parameters are evaluated by calculating the likelihood ratio of each point to the best fit point and are drawn in Fig. 4. The 90% C.L. contour crosses the  $\sin^2 2\theta = 1$  axis at  $\Delta m^2 = 1.9$  and  $3.6 \times 10^{-3} \text{ eV}^2$ . The oscillation parameters from the  $E_\nu$  spectrum distortion alone, or the total event analysis alone also agree.

In conclusion, using accelerator produced neutrinos, we see the same neutrino oscillation discovered with atmospheric neutrino measurements. This result is based on data from 1999 to 2004, a total of  $8.9 \times 10^{19}$  POT. The observed number of events and energy spectrum of neutrinos at SK are consistent with neutrino oscillation. The probability that we would see this result if there was

no oscillation is 0.0050% ( $4.0\sigma$ ). The allowed regions of the oscillation parameters from the K2K experiment are consistent with the atmospheric measurements.

We thank the KEK and ICRP directorates for their strong support and encouragement. K2K is made possible by the inventiveness and the diligent efforts of the KEK-PS machine group and beam channel group. We gratefully acknowledge the cooperation of the Kamioka Mining and Smelting Company. This work has been supported by the Ministry of Education, Culture, Sports, Science and Technology of the Government of Japan, the Japan Society for Promotion of Science, the U.S. Department of Energy, the Korea Research Foundation, the Korea Science and Engineering Foundation, NSERC Canada and Canada Foundation for Innovation, the Istituto Nazionale di Fisica Nucleare (Italy), the Spanish Ministry of Science and Technology, and Polish KBN grants: 1P03B08227 and 1P03B03826.

- 
- [1] Y. Ashie *et al.* [Super-Kamiokande Collaboration], Phys. Rev. Lett. **93**, 101801 (2004).
  - [2] M. Ambrosio *et al.* [MACRO Collaboration], Phys. Lett. **B566**, 35-44 (2003) .
  - [3] M. Sanchez *et al.* [Soudan2 Collaboration], Phys. Rev. D **68**, 113004 (2003)
  - [4] T. Araki *et al.* [KamLAND Collaboration], arXiv:hep-ex/0406035 .
  - [5] M. B. Smy *et al.* [Super-Kamiokande Collaboration], Phys. Rev. D **69**, 011104 (2004) .
  - [6] S. N. Ahmed *et al.* [SNO Collaboration], Phys. Rev. Lett. **92**, 181301 (2004) .
  - [7] Y. Fukuda *et al.* [Super-Kamiokande Collaboration], Phys. Rev. Lett. **81**, 1562 (1998) .
  - [8] S. H. Ahn *et al.* [K2K Collaboration], Phys. Lett. B **511**, 178 (2001)
  - [9] M. H. Ahn *et al.* [K2K Collaboration], Phys. Rev. Lett. **90**, 041801 (2003) .
  - [10] S. Fukuda, *et al.* [Super-Kamiokande Collaboration], Nucl. Instrum. Meth. **A501**, 418-462 (2003).
  - [11] A. Suzuki *et al.* [K2K Collaboration], Nucl. Instrum. Meth. A **453** 165 (2000) .
  - [12] B. J. Kim *et al.*, Nucl. Instrum. Meth. A **497** 450 (2003).
  - [13] T. Ishii *et al.* [K2K MRD Group], Nucl. Instrum. Meth. A **482**, 244 (2002) [Erratum-ibid. A **488**, 673 (2002)] .
  - [14] K. Nitta *et al.*, Nucl. Instrum. Meth., in press. [arXiv:hep-ex/0406023]
  - [15] D. Rein and L. M. Sehgal, Annals Phys. **133**, 79 (1981).
  - [16] D. Rein and L. M. Sehgal, Nucl. Phys. B **223**, 29 (1983).
  - [17] J. Marteau, J. Delorme and M. Ericson, Nucl. Instrum. Meth. A **451**, 76 (2000).